Tetrahedron 66 (2010) 6217–6223

Contents lists available at ScienceDirect

Tetrahedron

journal homepage: www.elsevier.com/locate/tet

Synthesis, photophysical properties, and cyanide detection in aqueous solution of **BF_2-curcumin** dyes

Anusak Chaicham [a], Sirinan Kulchat [a], Gamolwan Tumcharern [b], Thawatchai Tuntulani [a], Boosayarat Tomapatanaget [a,*]

[a] Supramolecular Chemistry Research Unit, Department of Chemistry, Faculty of Science, Chulalongkorn University, Bangkok, 10330, Thailand
[b] National Nanotechnology Center, National Science and Technology Development Agency, Pathumthani 12120, Thailand

ARTICLE INFO

Article history:
Received 8 February 2010
Received in revised form 4 May 2010
Accepted 24 May 2010
Available online 4 June 2010

ABSTRACT

Derivatives of difluoroboron curcumin (**BF_2-curcumin**, **BF_2-cur(OMe)$_2$**, **BF_2-cur(OTs)$_2$**, and **BF_2-curOTs**), were synthesized. All compounds possessed electron donor moieties at both ends of the conjugated π system and an electron acceptor moiety in the middle of the molecules (D–A–D system) and should exhibit different optical properties depending on substituents on the benzene rings. Photophysical properties of curcumin and difluoroboron curcumin derivatives were explored. The electron-withdrawing substituent could decrease the electron acceptability of BF_2-acceptor moiety resulting in the hypsochromic shift of both absorption and emission bands. **BF_2-curcumin** and **BF_2-cur(OMe)$_2$** displayed the positive solvatochromic effect relying predominantly on polarity and polarizability of the solvent. Interestingly, **BF_2-curcumin** showed high selectivity and sensitivity towards cyanide with the detection limits of 22 μM and 0.14 μM measured by visual detection and UV–vis spectrophotometry, respectively. Compared to the original curcumin, **BF_2-curcumin** offered a remarkably promising detection of cyanide with 66-fold enhancement in aqueous media (4:1 of CH_3CN/H_2O).

1. Introduction

In recent years, chemists have employed a number of dyes and their derivatives in colorimetric detection of toxic substances.[1] Curcumin, obtained by extraction of the rhizomes of *Curcuma Longa*, is a natural yellow-orange dye with low toxicity. Turmeric root is a well-known spice, cosmetic and medicine[2] due to its interesting multiple pharmacological effects, for examples, *anti*-oxidant, *anti*-cancer, *anti*-inflammatory, and potent *anti*-Alzheimer's disease activity.[3–9] Curcumin consists of two methoxy phenols conjugated through α,β-unsaturated β-diketone linker, which can perform a keto-enol tautomerism. A few investigations concerning photophysical properties of curcumin for medicinal chemistry have been reported.[10–12] Curcumin surprisingly exhibits many interesting photophysical and photochemical properties. The absorption band is approximately 408–430 nm in most organic solvents while the fluorescence spectrum is solvent-sensitive with emission wavelengths ranging from 460 to 560 nm.[13] Considering the fluorescent responses of curcumin, the emission quantum yield decreases on going from solvents of low polarity to those of high polarity. Recently, fluorescent borondifluoride dyes, such as bodipy[14–19] and boron/diketonates[20–24] have offered the advantages of optical properties including high emission quantum yields, large molar extinction coefficients and high sensitivity upon changes in solvent polarity.[25] In 1993, Montellano et al.[26] pioneered the addition of the difluoroboron moiety on the enolate group of curcumin and studied the inhibition of HIV-1 and HIV-2 proteases. Difluoroboron-curcumin displayed HIV-1 inhibition with IC_{50} of 24 μM while the typical curcumin showed HIV-1 inhibition with IC_{50} of 100 μM.

Cyanide, which was released in a widespread way from industrial uses, was found to cause severe toxicity in physiological system and environments. In the last decades, many efforts have been devoted to design various chemosensors specific for CN^- detection[27–30] since this method is outstanding in terms of inexpensive cost and rapid implementation. Yoon et al.[31] have collected and summarized researches involving optical sensors for cyanide based on a covalently linked binding site and signaling unit,[32,33] displacement approach of Cu complex and CN^-[34,35] and chemodosimeter of cyanide-substitution.[36,37] However, a significant visual change for cyanide sensing employing a deprotonation approach is still rare. Here, we aim to investigate the photophysical and photochemical properties of derivatives of **BF_2-curcumin**. Addition of BF_2 on the carbonyl group can inhibit the keto-enol tautomerization possibly resulting in an improvement in the photophysical properties and stability of curcumin.

* Corresponding author. Tel.: +662 2187642; fax: +662 2541309; e-mail address: tboosayarat@gmail.com (B. Tomapatanaget).

0040-4020/$ – see front matter Crown Copyright © 2010 Published by Elsevier Ltd. All rights reserved.
doi:10.1016/j.tet.2010.05.088

The **BF_2-curcumin** complexes consist of two methoxy phenol as electron donor parts conjugated to the difluoroboron enolate as the electron acceptor part resulting in a D–A–D system. In our design, the substituents on the OH moiety of **BF_2-curcumin** were synthetically modified to **BF_2-cur(OMe)$_2$**, **BF_2-cur(OTs)$_2$**, and **BF_2-cur OTs** in order to evaluate the effect of substituents on the photophysical properties of **BF_2-curcumin**. We explored the solvatochromic behavior of **BF_2-curcumin** and **BF_2-cur(OMe)$_2$** in various solvents. Moreover, we also investigated the cyanide sensing property of **BF_2-curcumin** in aqueous media compared with the original curcumin.

2. Results and discussion

2.1. Synthesis

All difluoroboron curcumin derivatives, **BF_2-cur(OMe)$_2$**, **BF_2-cur(OTs)$_2$**, and **BF_2-curOTs** were prepared from curcumin obtained by extraction of the rhizomes of *C. longa*. The synthesis of all compounds was illustrated in Scheme 1. **BF_2-curcumin**, was prepared by the addition of borontrifluoride diethyletherate to the enolate unit of curcumin.[25] **BF_2-cur(OMe)$_2$** was obtained by methylating **BF_2-curcumin** with methyl iodide using potassium carbonate as base. The ^{1}H NMR spectrum of **BF_2-cur(OMe)$_2$** displayed the methoxy protons at 3.82 ppm. The methoxy group in this compound was a representative of an electron-donating group.

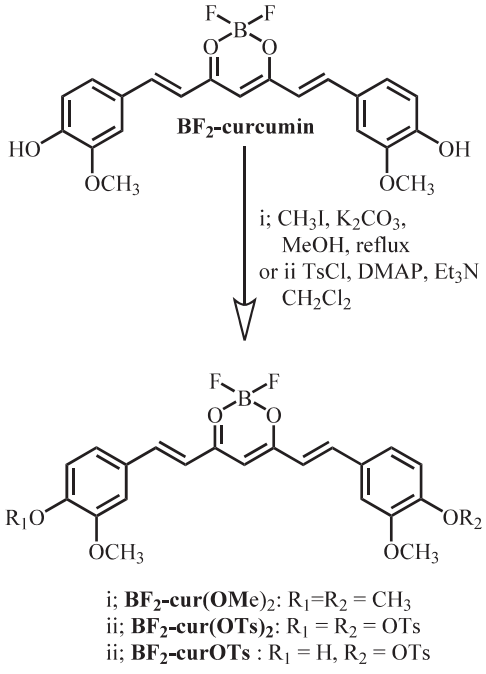

Scheme 1. Synthesis of **BF_2-cur(OMe)$_2$**, **BF_2-cur(OTs)$_2$** and **BF_2-curOTs**.

Mono and di-tosylated (**BF_2-curOTs** and **BF_2-cur(OTs)$_2$**) were prepared by the reaction between **BF_2-curcumin** and tosyl chloride. ^{1}H NMR spectra showed significantly different patterns between di- and mono-tosylation indicating by the ratio of 2:1 for the aromatic protons of the tosyl groups. The mono-tosyl compound displayed two non-equivalent methyl protons at different positions of 3.50–4.00 ppm. The purity of all prepared compounds was assured by the good agreement of elemental analysis except for **BF_2-curOTs**, which readily decomposed in air.

2.2. Photophysical properties of all difluoroboron curcumin derivatives

The photophysical behavior of all D–A–D molecules, **BF_2-cur(OMe)$_2$**, **BF_2-curOTs**, and **BF_2-cur(OTs)$_2$**, exhibited a strong absorption and emission band in CH_2Cl_2 as shown in Table 1. It was found that when the OH group was replaced with the electron-donating group such as OMe in **BF_2-cur(OMe)$_2$**, the maximum absorption spectrum of **BF_2-cur(OMe)$_2$** showed a small red shift at 502.1 nm ($\Delta\lambda_{max(ex)}$=5.1 nm in CH_2Cl_2) compared to that of **BF_2-curcumin**. This red shift is less than Moore's **CRANAD 2** ($\lambda_{max(ex)}$=760 nm in MeOH) containing a *N*′,*N*-dimethyl moiety instead of OH group on the ends of benzene rings leading to a large bathochromic shift.[38] Conversely, a blue shift of the absorption band was observed when the hydroxyl groups in **BF_2-curcumin** were modified with an electron-withdrawing group such as OTs in **BF_2-cur(OTs)$_2$** (Fig. 1a). Therefore, the substituted group influenced the electron accepting ability of the BF_2-part. Their relative transition energies should be dependent on the relative electron affinity of the donor fragment (curcumin part).[39] An electron-withdrawing group on the donor fragment will decrease the electron accepting ability of BF_2-part inducing the blue shift of the absorption band, while the electron-donating group will promote the electron accepting ability of the BF_2-part resulting in a red-shifted absorption band.

Table 1
Photophysical properties of **BF_2-curcumin**, **BF_2-cur(OMe)$_2$**, **BF_2-curOTs** and **BF_2-cur(OTs)$_2$** in CH_2Cl_2 at a concentration of 1.0×10^{-6} M

Compound	Absorption (nm)	Emission (nm)	Quantum yield	Molar absorptivity ($\times10^5$ cm^{-1} mol^{-1} L)
BF_2-curcumin	497	557.01	0.62	0.82
BF_2-cur(OMe)$_2$	502.1	570.00	0.61	1.29
BF_2-curOTs	492.0	562.00	0.22	0.33
BF_2-cur(OTs)$_2$	436.0, 460.1	505.07	0.48	0.34

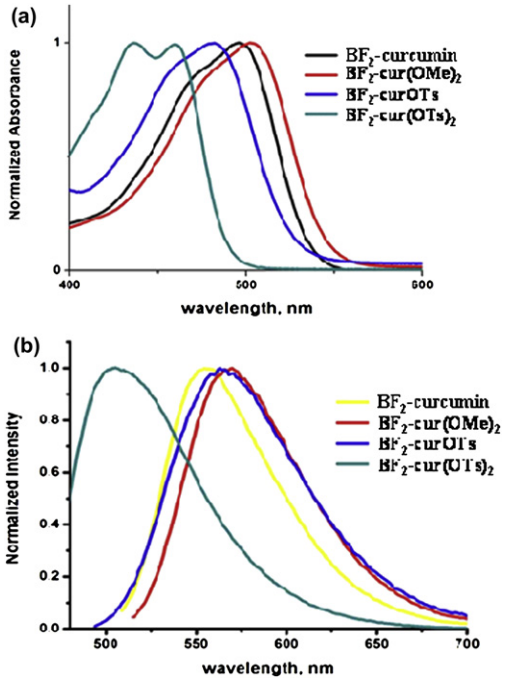

Figure 1. The normalized UV–vis spectra (a) and fluorescence spectra (b) of **BF_2-curcumin**, **BF_2-cur(OMe)$_2$**, **BF_2-curOTs** and **BF_2-cur(OTs)$_2$** in CH_2Cl_2 at a concentration of 1.0×10^{-3} mM.

Compared to **BF_2-curcumin**, the emission spectra of **BF_2-curOTs** and **BF_2-cur(OMe)$_2$** demonstrated a trend of a small red shift depending on the electron accepting ability of the BF_2-part. **BF_2-curOTs**, however, showed the maximum emission wavelength of 562 nm, which is higher than that of **BF_2-curcumin** (557.10 nm) (Fig. 1b). The unsymmetrical structure of **BF_2-curOTs** with different

substituents on both ends of benzene rings causes a higher relaxation of electrons resulting in the bathochromic shift compared to **BF_2-curcumin**.

2.3. Studies of solvatochromic effects of difluoroboron curcumin derivatives

BF_2-curcumin and **BF_2-cur(OMe)$_2$** are soluble in several common organic solvents and exhibit solvent-dependent photophysical properties in selected common organic solvents (Fig. 2). It was worth noting that the color of the solutions changed ranged from yellow to red on going from solvents of low polarity to those of high polarity. **BF_2-curcumin** in selected solvents exhibited different colors with a red colorshade upon increasing the solvent polarity and a very bright fluorescent emission with low solvent polarity (Fig. 2a and Fig. 2b). The normalized UV–vis and fluorescence spectra of **BF_2-curcumin** in several organic solvents are shown in Figures 3a and b. The fluorescent quantum yields of **BF_2-curcumin** and **BF_2-cur(OMe)$_2$** were collected in Tables S1 and S2. The results can be rationalized that the increase of the electron accepting ability of the BF_2-acceptor enhanced the charge separation or dipole-moment of the molecule. Therefore, the different solvent polarities yielded different colors of the solution.

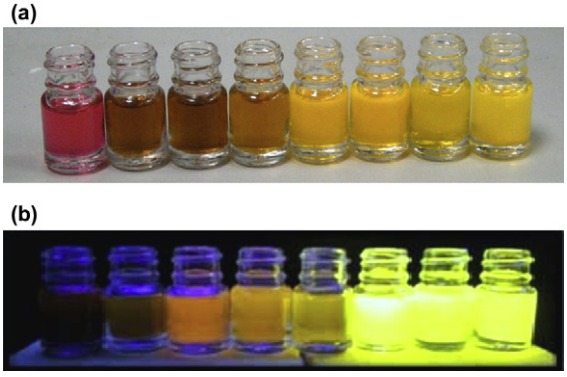

Figure 2. The photographs of **BF_2-curcumin** in organic solvents (from left to right, DMSO, CH_3OH, CH_3Cl, C_2H_5OH, CH_3CN, CH_2Cl_2, EtOAc, and *o*-$C_6H_4Cl_2$) under illumination of (a) white light and (b) black light (λ=365 nm).

To explain the solvent effect on the photophysical properties of **BF_2-curcumin** and **BF_2cur(OMe)$_2$**, the linear solvation energy relationships (LSER) based on the Kamlet–Taft equation were examined. The solvatochromic parameters involving π^* (polarity/polarizability factor), α (solvent hydrogen bond donor ability, HBD), and β (solvent hydrogen bond acceptance ability, HBA) are used in the Kamlet–Taft relationship as shown in Eq.1.[40]

$$y = y_0 + a\alpha + b\beta + c\pi^* \quad (\text{Kamlet} - \text{Taft}) \tag{1}$$

The coefficients (y_0, a, b, and c), and correlation coefficients (R^2) were evaluated by multiple linear regression fit to the Kamlet–Taft relationship of the absorption spectra of **BF_2-curcumin** and **BF_2-cur(OMe)$_2$**, and summarized in the Supplementary data. The solvents used in this study were CH_3OH, DMSO, C_2H_5OH, $CHCl_3$, C_6H_6, $CH_3C_6H_5$, and $(CH_3CH_2)_2O$. The solvatochromic parameters expressed in Eqs. 2 and 3 were obtained from the best linear regression fits[40] between the calculated and measured

ν_{max} with R^2 values of 0.991 and 0.997 for **BF_2-curcumin** and **BF_2-cur(OMe)$_2$**, respectively (Fig. 4 and Fig. S5).

$$\tilde{\nu}_{\max}\text{BF2} - \text{curcumin}\left(x10^{-3}\right) = 20.97 + 0.23\alpha - 0.70\beta - 1.39\pi^* \tag{2}$$

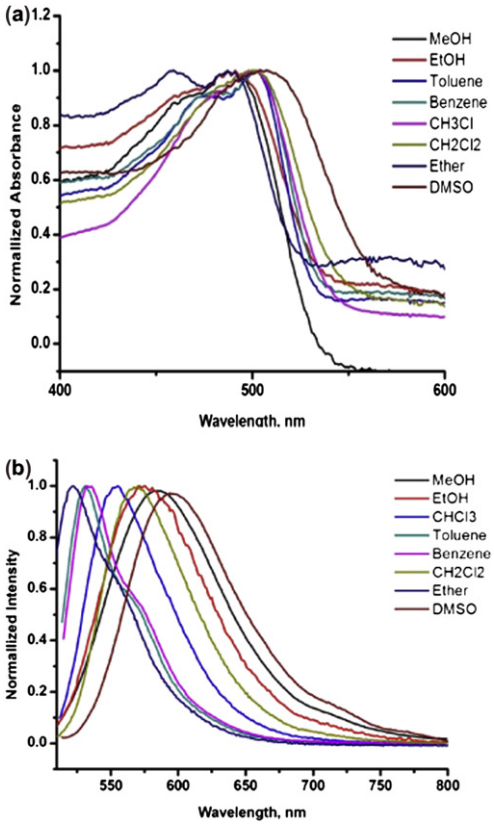

Figure 3. The normalized UV–vis spectra (a) and fluorescence spectra (b) of **BF_2-curcumin** in various organic solvents.

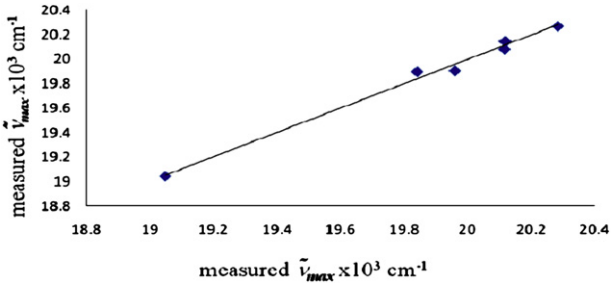

Figure 4. Multi-parameter linear regression analysis between calculated and measured absorption of **BF_2-curcumin**.

$$\tilde{\nu}_{\max}\text{BF2} - \text{curcumin}\left(x10^{-3}\right) = 20.61 + 0.39\alpha + 0.20\beta - 1.32\pi^* \tag{3}$$

From Eqs. 2 and 3, the polarity/polarizability factors (π^*) play the most important role on the photophysical properties of **BF_2-curcumin** and **BF_2-cur(OMe)$_2$**. Additionally, hydrogen bond accepting abilities (β) followed by hydrogen bond donating abilities (α) play a minor effect for the former derivative. This result implied that the dipole/dipole interaction between the curcumin derivatives and the medium is markedly larger than the hydrogen bonding between the solute and the solvent. The '*c*' values are minus for **BF_2-curcumin** and **BF_2-cur(OMe)$_2$**, indicating the electronically excited state of these molecules with a stronger solvate stabilized upon increasing the solvent's dipolarity/polarizability resulting in a good agreement with bathochromic shift of UV–vis absorption maxima on going from benzene to DMSO. Considering in each coefficient, '*a*' and '*c*' are approximately the same in both **BF_2-curcumin** and **BF_2-cur(OMe)$_2$** systems, while '*b*' displays large difference. This result suggested that

HBA plays a larger role than HBD in the photophysical properties of both curcumin derivatives in organic solvents. It is also worth mentioning that the negative value of HBA of **BF_2-curcumin** in organic solvent indicates the favorable hydrogen bonding towards a protophilic solvent leading to the bathochromic shift of the absorption band.[41] On the contrary, the coefficient of the HBA part in the Kamlet–Taft equation of **BF_2-cur(OMe)$_2$** system means unfavorable hydrogen bond interaction in a protic solvent. Undoubtedly, the maximum absorption of **BF_2-cur(OMe)$_2$** in methanol and ethanol illustrated a blue shift of ~13 nm compared with the solution in benzene (see in Supplementary data). The unfavorable hydrogen bond interaction in a protic solvent of **BF_2-cur(OMe)$_2$** related to the fluctuation of the maximum absorption in the optical spectra with an increase of the solvent polarity. However, **BF_2-curcumin** and **BF_2-cur(OMe)$_2$** generally displayed a positive solvatochromism under the effect of solvent dipolarity/polarizability factor.

2.4. Anion sensing of BF_2-curcumin and curcumin

The complexed properties of **BF_2-curcumin** towards anions, in comparison with **curcumin**, were investigated. All optical and emission spectrum were measured in CH_3CN/H_2O (4:1 v/v), since deprotonation by a strongly basic anion might occur at the hydroxyl group of both compounds. Anion sensing ability of **BF_2-curcumin** was examined with various anions (F^-, Cl^-, Br^-, I^- CN^-, AcO^-, and BzO^-, and $H_2PO_4^-$) by UV–vis and fluorescence spectrophotometry.

Upon addition of CN^-, the color transitions from red to blue of **BF_2-curcumin** and from yellow to red of **curcumin** were observed by naked-eye (Fig. 5). For other anions, the color of solution remained unchanged. The photophysical properties were further examined by UV–vis spectrophotometry. The absorption band of **BF_2-curcumin** at 507 nm decreased concurrently with the appearance of a new strong absorption band at 649 nm in the presence of CN^- (Fig. 6). In the case of AcO^- and BzO^-, the maximum absorption at 507 nm slightly decreased, and a weak absorption band at 625 nm intensified. No spectrum change was observed for F^-, Cl^-, Br^-, I^-, and $H_2PO_4^-$. The addition of CN^- in the **curcumin** solution leaded to a bathochromic shift (from 460 to 510 nm). In the case of the other anions, the UV–vis spectrum remained unchanged (shown in S7).

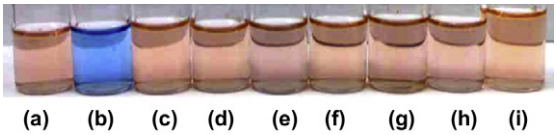

Figure 5. Color transition of A. **BF_2-curcumin** (1.0×10^{-6} M) in CH_3CN/H_2O (4:1, v/v) solution in the presence of 100 equiv of various anions (a) none, (b) CN^-, (c) F^-, (d) Br^-, (e) Cl^-, (f) I^-, (g) BzO^-, (h) AcO^-, and (i) H_2PO_4.

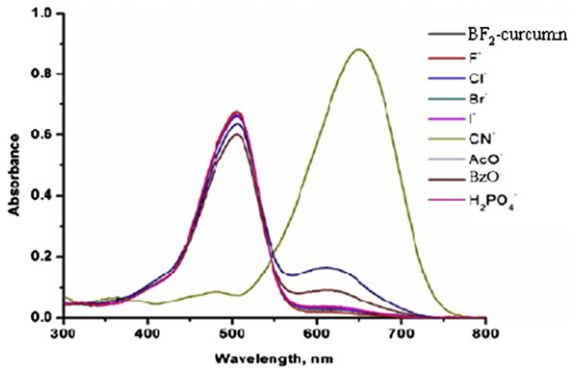

Figure 6. UV–vis spectra of **BF_2-curcumin** (5 μM) in CH_3CN/H_2O (4:1, v/v) in the presence of 100 equiv of various anions.

Photoemission properties of **BF_2-curcumin** and curcumin were also investigated. The fluorescent spectrum of **BF_2-curcumin** showed a strong emission band at 600 nm while that of curcumin displayed a very weak emission band at 543 nm as shown in Figure 7. Compared to curcumin, a large red shift and high quantum yield of **BF_2-curcumin** could stem from the electron transition from π to π* from oxygen to the empty orbital of boron.[42] The incorporation of BF_2 on the curcumin structure resulted in a more rigid structure and extended π-conjugation and consequently facilitated electron transfer through the conjugated system.

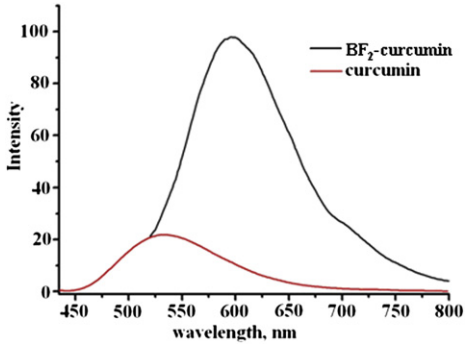

Figure 7. Fluorescent spectra of **BF_2-curcumin** and **curcumin** in CH_3CN/H_2O (**4**:**1** v/v).

The emission spectra of **BF_2-curcumin** and **curcumin** in the presence of various anions are illustrated in Figure 7. Interestingly, excitation wavelength dependent fluorescence spectra were observed. The emission bands of **BF_2-curcumin** in the presence of CN^- were markedly changed. The excitation wavelength of 507 nm resulted in a complete quenching at the emission wavelength of 600 nm. On the other hand, a new emission band at 750 nm of the cyanide complex appeared upon changing the excitation wavelength to 649 nm (Fig. 8, inset). In the case of other anions, the emission bands at 649 nm slightly change without the appearance of a new emission band at 750 nm when excited at 649 nm. The fluorescence responses of **curcumin** towards various anions were also investigated.

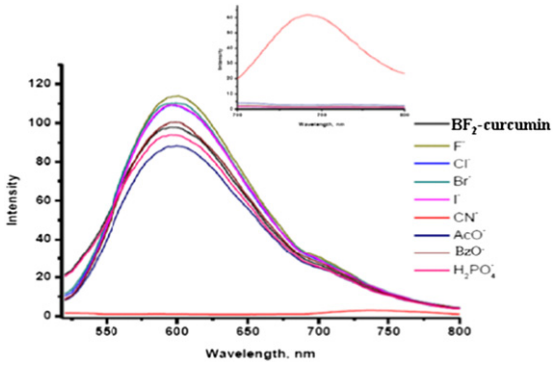

Figure 8. Fluorescent spectra of **BF_2-curcumin** with various anions (λ_{ex}=507 nm, Inset: λ_{ex}=649 nm).

The presence of cyanide in the solution of curcumin caused a complete quenching of the emission band at 543 nm without the appearance of a new emission band. No changes were observed with other anions. (Fig. S14 in Supplementary data).

The photophysical and photochemical phenomena of **BF_2-curcumin** in the presence of cyanide were assumed to undergo the deprotonation of hydroxyl groups by CN^-. NMR spectra showed a strong evidence to support this assumption (Fig. 9). According to ^{1}H NMR spectra of **BF_2-curcumin** and CN^-, the hydroxyl protons

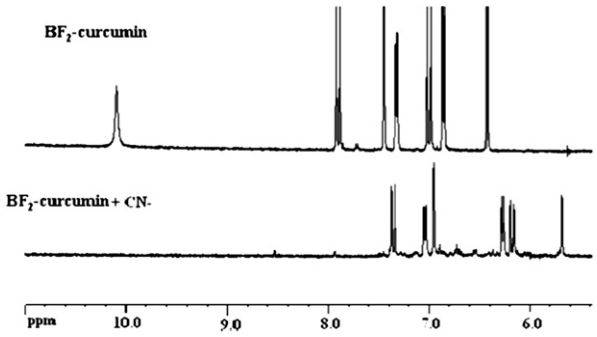

Figure 9. ^{1}H NMR spectrum of **BF_2-curcumin** and **BF_2-curcumin**+CN^- in DMSO-d_6.

(10.09 ppm) completely disappeared with a concomitant of the large upfield shifts of aromatic and alkene protons from 7.90–6.42 to 7.28–5.64 ppm. This indicated that the aromatic protons were shielded by the negative charge of the deprotonated hydoxyl group.

This deprotonation caused a high charge separation between acceptor and donor unit in **BF_2-curcumin**, and consequently excellent electron delocalization to **BF_2** unit. The excited states in the complexes were stabilized upon the binding of CN^-, resulting in a bathochromic shift in the absorption band with $\Delta\lambda$=142 and 92.9 nm for **BF_2-curcumin** and **curcumin**, respectively. Moreover, a new emission band at 750 nm for **BF_2-curcumin** and CN^- was observed. The red shift of **BF_2-Curcumin** is larger than that of **curcumin**, possibly caused by a large charge separation between **BF_2** unit and the aromatic rings resulting in a strong intramolecular charge transfer (ICT).[43–46] A schematic illustration is shown in Scheme 2.

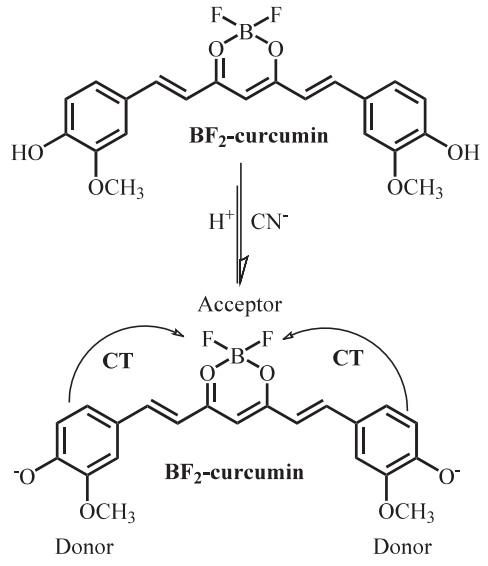

Scheme 2. The ICT process of **BF_2-curcumin** upon adding CN^-.

The selective binding properties of **BF_2-curcumin** and **curcumin** towards CN^- can be described by the basicity of anions. The charge transfer process could not occur in the case of fluoride ion due to its high hydration enthalpy and low basicity (ΔH^0_{hyd}=−504 kJ/mol, pK_a=3.18) in an aqueous system.[47] Furthermore, the binding constants of **BF_2-curcumin** or **curcumin** towards CN^- were carried out by UV–vis and fluorometric titrations. Logarithm (log β_2)[48] of overall stability constants of the deprotonation of **BF_2-curcumin** are 8.8 and those of **curcumin** are 7.7.

The interference of foreign substances; such as, F^-, Cl^-, Br^-, I^-, AcO^-, BzO^-, and $H_2PO_4^-$ against cyanide detection of **BF_2-curcumin** and **curcumin** was evaluated by fluorescence methods. Compared to curcumin, the presence of the BF_2 part in **BF_2-curcumin** showed a benefit on the reduction of the interference effect from other anions (Fig. 10). The fluorescence signal of the solution of **curcumin** and cyanide were seriously disturbed by other anions. In the case of **BF_2-curcumin**, the miscellaneous competitive anions did not perturb the emission signal, except for F^-, AcO^-, and $H_2PO_4^-$ The tolerance of cyanide sensing against other interference anions, in which the relative error are fixed at ±10%,[49] was listed in Table S5. The presence of F^-, AcO^-, and $H_2PO_4^-$ at molar ratios of 100, 470, and 6, respectively, could interfere the cyanide sensing of **BF_2-curcumin**.

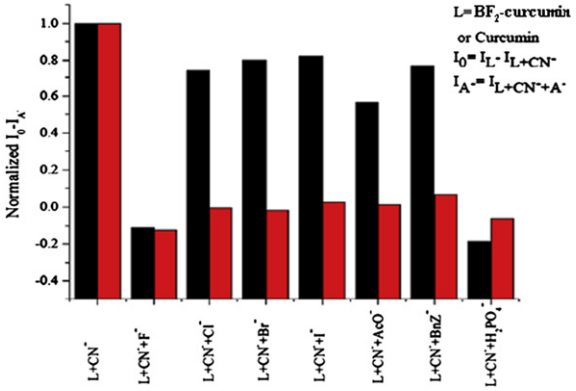

Figure 10. Fluorescence responses of **BF_2-curcumin** (black bar) and **curcumin** (red bar) (7.5 μM) to CN^- (0.5 mM.) in the presence of foreign anions in CH_3CN/H_2O (4:1) (**BF_2-curcumin**: λ_{ex}=507 nm, λ_{em}=600 nm, and **curcumin**: λ_{ex}=417.1 nm, λ_{em}=543 nm).

Colorimetric and UV–vis detection limits of **BF_2-curcumin** and **curcumin** for CN^- were also evaluated (Fig. 11). In CH_3CN/H_2O (4:1 v/v), the visual detection limit of **BF_2-curcumin** (10 μM) towards CN^- is 22 μM while in the case of **curcumin** (10^{-4} M), the color change can be detected visually at the concentration of CN^- ≥75 μM. Compared to the UV–vis detection limit, the absorption changes (Fig. 12), calculated on the basis of $3\sigma/K$,[50,51] could extend the limit of detection down to 0.14 and 9.33 μM for **BF_2-curcumin** and **curcumin**, respectively (Fig. 11).

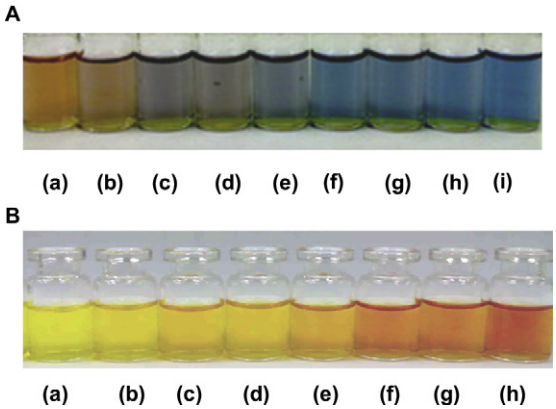

Figure 11. Colorimetric changes of A. **BF_2-curcumin** (0.01 mM) in CH_3CN/H_2O (4:1, v/v) upon the addition of (a) 0, (b) (15), (c) 22, (d) 24, (e) 29, (f) 36, (g) 43, (h) 50, and (i) 57 μM of CN B. **curcumin** (0.1 mM) in CH_3CN/H_2O (4:1, v/v) upon the addition of (a) 0, (b) 50, (c) 75, (d) 99, (e) 109, (f) 124, (g) 149, and (h) 172 μM of CN^-.

This is indicative of a higher detectable sensitivity of **BF_2-curcumin** than that of **curcumin** for cyanide sensing. Therefore, **BF_2-curcumin** is a promising sensor for cyanide. For **BF_2-curOTs**, we did not study the cyanide detection properties of this compound because it readily decomposed in air.

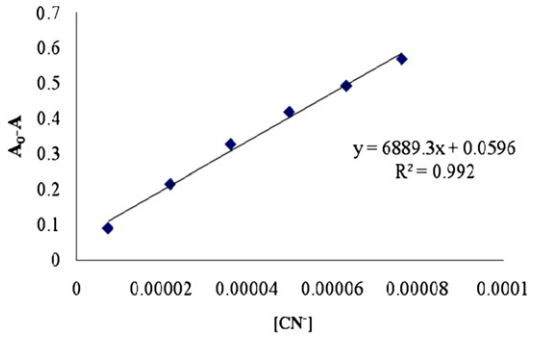

Figure 12. Linear plot between absorbance of **BF_2-curcumin** (7.5 μM) versus concentration of CN^-.

3. Conclusions

In summary, D–A–D molecular sensors employing derivatives of **BF_2-curcumin** with different substituents on hydroxyl groups were successfully synthesized, and their photo-physical and -chemical properties were examined. Electron-withdrawing substituted groups attached to the donor part of **BF_2-curcumin** induced a hypsochromic shift in both absorption and emission spectra. Conversely, electron-donating groups stabilized a higher energy level of the molecules resulting in the bathochromic shift of UV–vis and fluorescence spectra. The photophysical properties of **BF_2-curcumin** and **BF_2-cur(OMe)$_2$** exhibited a positive solvatochromic effect, mainly depending on the solvent polarity/polarizability factor. The incorporation of BF_2 on the curcumin structure gave a cyanide sensor with excellent selectivity and sensitivity. The sensing approach relied on the deprotonation of the hydroxyl group of **BF_2-curcumin** by CN^- leading to an extended π-conjugated system. **BF_2-curcumin** thus serves as a promising chemical sensor for cyanide detection by either naked-eye for on-site detection or spectrophotometry when a better resolution is required.

4. Experimental

4.1. Materials and methods

Nuclear magnetic resonance (NMR) spectra were recorded in DMSO-d_6, $CDCl_3$ and CD_3CN on a Varian 400 MHz spectrometer. Electrospray mass spectra were determined on a Micromass Platform quadrupole mass analyzer with an electrospray ion source using acetonitrile as solvent Elemental analyses were carried out on a Perkin–Elmer CHON/S analyzer (PE 2400 series II). Absorption spectra were measured by a Varian Cary 50 UV–vis spectrophotometer. Fluorescence spectra were performed on a Varian eclipse spectrofluorometer. Unless otherwise specified, the solvents and all materials were reagent grades without further purification. Commercial grade solvents such as acetone, dichloromethane, hexane, methanol, and ethyl acetate were purified by distillation. Acetonitrile, dimethylformamide, and dichloromethane were dried over calcium hydride and THF was dried over benzoquinone and sodium and freshly distilled under nitrogen prior to use.

4.2. Synthesis

*4.2.1. Preparation of methylated curcumin borondifluoride (**BF_2-cur(OMe)$_2$**).* In a 250 mL two-necked round bottom flask equipped with a magnetic bar and a reflux condenser, a solution of **BF_2-curcumin** (0.416 g, 1 mmol) and anhydrous potassium carbonate in methanol (100 ml) was stirred for 10 min. Methyl iodide (1.5 mL, 2 mmol) in methanol (4 mL) was added dropwise into the reaction mixture, which was refluxed at 60 °C overnight. The solvent was removed by rotary evaporator to obtain a crude product. The crude product was dissolved in ethyl acetate and washed with water. The organic layer was dried over anhydrous sodium sulfate and evaporated to dryness under reduced pressure. The desired product (**BF_2-cur(OMe)$_2$**) was obtained as a purple crystalline solid (73% yield) after recrystallization in hexane/ethyl acetate. ^{1}H NMR (400 MHz, DMSO) δ (in ppm)=7.954 (J=16.0 Hz, d, –Ar*H*, 2H), 7.477 (s, –Ar*H*, 2H,), 7.450 (J=8.4 Hz, d, –Ar*H*, 2H), 7.086 (J=15.6 Hz, d, –olifinic-*H*, 2H,), 7.077 (s, –Ar*H*, 2H), 6.487 (s, –Ar*H*, 1H), 3.822 (s, –O*CH*$_3$, 12H,). ^{13}C NMR (100.6 MHz, $CDCl_3$) δ (in ppm)=56.11, 56.22, 102.20, 111.63, 112.23, 119.30, 125.64, 127.54, 147.28, 149.55, 153.01, 179.50; ESI MS: m/z=445.63 [M^+]. Anal. Calcd for $C_{23}H_{15}N_3O_3$: C, 62.18; H, 5.22. Found: C, 62.53; H, 5.32.

*4.2.2. Preparation of monotosylation curcumin borondifluoride (**BF_2-curOTs**) and ditosylation curcumin borondifluoride (**BF_2-cur(OTs)$_2$**).* In a 100 mL two-neck round bottom flask, a solution of **BF_2-curcumin** (0.277 g, 0.67 mmol), DMAP (4-Dimethylaminopyridine), and triethylamine (0.084 mL, 2.01 mmol) was stirred for 30 min in dichloromethane (30 mL) at 0 °C under nitrogen. A solution of *para*-toluenesulfonyl chloride (0.284 g, 1.49 mmol) in dichloromethane (10 mL) was added dropwise into the mixture over 30 min. Upon completion of the reaction, a solution of HCl (3 M) was added into the mixture to adjust the pH to 1 and stirred for 30 min. The reaction was extracted with water, and the organic solvent was dried over Na_2SO_4 and then evaporated in vaccuo. The crude product was purified by column chromatography using 5% ethyl acetate in dichloromethane to afford **BF_2-curOTs** (R_f=0.65) and **BF_2-cur(OTs)$_2$** (R_f=0.83) in 23% and 71% yields, respectively.

*4.2.2.1. **BF_2-curOTs**.* ^{1}H NMR (400 MHz, DMSO-d_6) δ (in ppm)= 7.97 (J=15.6 Hz, d, olifinic-*H*, 1H), 7.85 (J=15.2 Hz, d, olifinic-*H*, 1H), 7.70 (J=8.0 Hz, d, –ArH, 2H), 7.26 (J=8 Hz, d, –ArH, 2H), 7.07 (d, –ArH, 2H), 7.03 (s, –ArH, 1H), 6.93 (d, –ArH, 1H), 6.90 (s, –ArOH, 1H), 6.54 (J=15.6 Hz, d, –CH=CH–, 3H), 6.01 (J=17.2 Hz, d, –CH=CH–, 2H), 3.90 (s, –OCH_3, 3H), 3.56 (s, –OCH_3, 3H), 1.98 (s, –CH_3, 3H). ^{13}C NMR (100.6 MHz, $CDCl_3$) δ (in ppm)=29.71, 55.72, 56.07, 110.82, 112.83, 115.46, 121.39, 121.62, 124.46, 124.69, 128.61, 129.50, 133.93, 139.24, 145.03, 147.13, 148.82, 180.01; ESI MS: m/z=570.87 [M^+] ($C_{23}H_{23}BF_2O_6$)

*4.2.2.2. **BF_2-cur(OTs)$_2$**.* ^{1}H NMR (400 MHz, DMSO-d_6) 7.91 (J=16 Hz, d, olifinic-*H*, 2H), 7.70 (J=8.4 Hz, d, –Ar*H*, 4H), 7.26 (J=8.0 Hz, d, –Ar*H*, 4H), 7.15 (d, –Ar*H*, 4H), 6.96 (s, –C*H*=C*H*–, 2H), 6.59 (J=15.6 Hz, d, –C*H*=C*H*–, 2H), 6.04 (s, –C*H*=C*H*–, 1H), 3.57 (s, –O*CH*$_3$, 6H), 2.40 (s, –C*H*$_3$, 6H). ^{13}C NMR (100.6 MHz, $CDCl_3$) δ (in ppm)=21.76, 55.74, 102.56, 112.91, 121.34, 121.67, 124.74, 128.59, 129.55, 133.0, 133.73, 140.92, 145.48, 146.38, 152.35, 180.06; HRMS (positive ESI) m/z calcd for $C_{23}H_{23}BF_2O_6Na$ ($M+Na^+$) 747.1420, found 747.1396.

4.3. Studies of solvent effects of BF_2-curcumin and BF_2-cur(OMe)$_2$

The solutions of **BF_2-curcumin** and **BF_2-cur(OMe)$_2$** (1.0 mM) were prepared in organic solvents (spectroscopic grade), such as methanol, ethanol, toluene, benzene, chloroform, dichloromethane, diethyl ether, ethyl acetate, and DMSO and were placed in 10.0 mm width quartz cell. Fluorescence spectra (excitation at 497.1 and 503.0 nm for **BF_2-curcumin** and **BF_2-cur(OMe)$_2$**, respectively) and UV–vis spectra were recorded at room temperature.

4.4. UV–vis titrations and fluorescent titrations to determine the binding constants of BF_2-curcumin and curcumin towards CN^-

All UV–vis and fluorescent titrations of **BF_2-curcumin** (7.5×10^{-3} mM) and **curcumin** (5.0×10^{-3} mM) in the presence of cyanide ion were recorded in CH_3CN/H_2O (4/4 v/v) using of [Bu4N][PF6] (0.01 M) as a supporting electrolyte. The solutions of CN^- were prepared and gradually added into the solution of receptor (2 mL). Absorption and emission spectra of solution were recorded after each addition until absorbance of a new peak at 649 nm and 510 nm and emission quenching at 600 nm and 543 nm for **BF_2-curcumin** and **curcumin**, respectively, were constant. The stability constants (log β) of cyanide complexes of receptors were evaluated by fitting the titration curves to the non-linear relation using the following equations (Eqs. 4 and 5 for fluorescence and UV–vis techniques, respectively).

$$I = \frac{I_0 + I_\infty \beta_n \left[CN^-\right]^n}{1 + \beta_n \left[CN^-\right]^n} \quad (4)$$

$$A = \frac{A_0 + A_\infty \beta_n \left[CN^-\right]^n}{1 + \beta_n \left[CN^-\right]^n} \quad (5)$$

Acknowledgements

AC is a M.Sc. student supported by Thailand Graduate Institute of Science and Technology (TGIST) and SK is a M.Sc. student supported by Junior Science Talent Project (JSTP). The authors wish to thank the grants provided by National Nanotechnology Center (NN-B-22-b15-94-49-55) and the Thailand Research fund (RTA5080006). The authors also appreciate THAI-CHINA FLAVORS & FRAGRANCES INDUSTRY CO., LTD for providing the turmeric extract (curcumin powder).

Supplementary data

The analysis of the synthesized compounds including NMR spectra, UV–vis and fluorescent experiments are provided. Supplementary data associated with this article can be found in online version at doi:10.1016/j.tet.2010.05.088.

References and notes

1. Tomasulo, M.; Raymo, M. F. *Org. Lett.* **2005**, *7*, 4633–4636.
2. Chattopadhyay, I.; Biswas, K.; Bandyopadhyay, U.; Banerjee, R. K. *Curr. Sci.* **2004**, *87*, 44–53.
3. Aggarwal, B. B.; Shishodia, S. *Biochem. Pharmacol.* **2006**, *71*, 1397–1421.
4. Leyon, P. V.; Kuttan, G. *J. Exp. Clin. Cancer Res.* **2003**, *22*, 77–83.
5. Nurfinal, A. N.; Reksohadiprodjo, M. S.; Timmerman, H. U.; Jenie, A.; Sugiyant, D.; van der Goot, H. *Eur. J. Med. Chem.* **1997**, *32*, 321–328.
6. Shishodia, S.; Sethi, G.; Aggarwal, B. B.; Ann, N. Y. *Acad. Sci.* **2005**, *1056*, 206–217.
7. Siwak, D. R.; Shishodia, S.; Aggarwal, B. B.; Kurzrock, R. *Cancer* **2005**, *104*, 879–890.
8. Aggarwal, B. B.; Shishodia, S.; Takada, Y.; Banerjee, S.; Newman, R. A.; Bueso-Ramos, C. E.; Price, J. E. *Clin. Cancer Res.* **2005**, *11*, 7490–7498.
9. Aggarwal, S.; Ichikawa, H.; Takada, Y.; Sandur, S. K.; Shishodia, S.; Aggarwal, B. B. *Mol. Pharmacol.* **2006**, *69*, 195–206.
10. Garcia-Alloza, M.; Borrelli, L. A.; Rozkalne, A. B.; Hyman, T. B.; Bacskai, J. *J. Neurochem.* **2007**, *102*, 1095–1104.
11. Yang, F.; Lim, G. P.; Begum, A. N.; Ubeda, O. J.; Simmons, M. R.; Ambegaokar, S. S.; Chen, P. P.; Kayed, R.; Glabe, C. G.; Frautschy, S. A.; Cole, G. M. *J. Biol. Chem.* **2005**, *280*, 5892–5901.
12. Ryu, E. K.; Choe, Y. S.; Lee, K. H.; Choi, Y.; Kim, B. T. *J. Med. Chem.* **2006**, *49*, 6111–6119.
13. Barik, A.; Priyadarsini, K. I.; Mohan, H. *Photochem. Photobiol.* **2003**, *77*, 597–603.
14. Priyadarsini, K. I. *J. Photochem. Photobiol. C: Photochem. Revs.* **2009**, *10*, 81–95.
15. Loudet, A.; Burgess, K. *Chem. Rev.* **2007**, *107*, 4891–4932.
16. Fana, J.; Guoa, K.; Penga, X.; Dua, J.; Wangb, J.; Suna, S.; Li, H. *Sens. Actuators, B* **2009**, *142*, 191–196.
17. Meng, G.; Velayudham, S.; Smith, A.; Luck, R.; Liu, H. *Macromolecules* **2009**, *42*, 1995–2001.
18. Donuru, V. R.; Vegesna, G. K.; Velayudham, S.; Green, S.; Liu, H. *Chem. Mater.* **2009**, *21*, 2130–2138.
19. Lai, R. Y.; Bard, A. J. *J. Phys. Chem. B* **2003**, *107*, 5036–5042.
20. Ma, G.; Cheng, Q. *Langmuir* **2006**, *22*, 6743–6745.
21. Chow, Y. L.; Johansson, C. I.; Zhang, Y.-H.; Gautron, R.; Yang, L.; Rassat, A.; Yang, S.-Z. *J. Phys. Org. Chem.* **1996**, *9*, 7–16.
22. Hales, J. M.; Zheng, S.; Barlow, S.; Marder, S. R.; Perry, J. W. *J. Am. Chem. Soc.* **2006**, *128*, 11362–11363.
23. Chow, Y. L.; Johansson, C. I. *J. Phys. Chem.* **1995**, *99*, 17558–17565.
24. Cogne'-Laage, E.; Allemand, J.-F.; Ruel, O.; Baudin, J.-B.; Croquette, V.; Blanchard-Desce, M.; Jullien, L. *Chem.—Eur. J.* **2004**, *10*, 1445–1455.
25. Pfister, A.; Zhang, G.; Zareno, J.; Horwitz, A. F.; Fraser, C. L. *ACS Nano* **2008**, *2*, 1252–1258.
26. Suai, Z.; Salto, R.; Li, J.; Craik, C.; Ch-tizde Montellano, P. R. *Bioorg. Med. Chem.* **1993**, *1*, 415–422.
27. Li, Z.; Lou, X.; Yu, H.; Li, Z.; Qin, J. *Macromolecules* **2008**, *41*, 7433–7439.
28. Sessler, J. L.; Cho, D.-G. *Org. Lett.* **2008**, *10*, 73–75.
29. Ho, H. A.; Leclerc, M. *J. Am. Chem. Soc.* **2003**, *125*, 4412–4413.
30. Powell, S. C. *Anal. Chem.* **2009**, *81*, 9535.
31. Xu, Z.; Chen, X.; Kim, H. N.; Yoon, J. *Chem. Soc. Rev.* **2010**, *39*, 127–137.
32. Anzenbacher, P., Jr.; Tyson, D. S.; Jurskova, K.; Castellano, F. N. *J. Am. Chem. Soc.* **2002**, *124*, 6232–6233.
33. Kim, Y.-H.; Hong, J.-I. *Chem. Commun.* **2002**, 512–513.
34. Ganesh, V.; Sanz, M. P. C.; Mareque-Rivas, J. C. *Chem. Commun.* **2007**, 5010–5012.
35. Zeng, Q.; Cai, P.; Li, Z.; Qina, J.; Tang, B. Z. *Chem. Commun.* **2008**, 1094–1096.
36. Kim, Y. K.; Lee, Y.-H.; Lee, H.-Y.; Kim, M.-K.; Cha, G. S.; Ahn, K. H. *Org. Lett.* **2003**, *5*, 4003–4006.
37. Ekmekci, Z.; Yilmaz, M. D.; Akkaya, E. U. *Org. Lett.* **2008**, *10*, 461–464.
38. Ran, C.; Xu, X.; Raymond, S. B.; Ferrara, B. J.; Neal, K.; Bacskai, B. J.; Medarova, Z.; Moore, A. *J. Am. Chem. Soc.* **2009**, *131*, 15257–15261.
39. Lakowicz, J. R. *Principles of Fluorescence Spectroscopy*; Spinger Science+Business Media, LLC: New York, NY, USA, 2006.
40. Marcus, Y. *Chem. Soc. Rev.* **1993**, *22*, 409–416.
41. Schreiter, K.; Spange, S. *J. Phys. Org. Chem.* **2008**, *21*, 242–250.
42. Roth, H. J.; Miller, B. *Arch. Pharm. Ber. Dtsch. Pharm. Ges.* **1964**, *297*, 660–673.
43. Huh, J. O.; Do, Y.; Lee, M. H. *Organometallics* **2008**, *27*, 1022–1025.
44. Marcotte, N.; Plaza, P.; Lavabre, D.; Fery-Forgues, S.; Martin, M. M. *J. Phys. Chem. A* **2003**, *107*, 2394–2402.
45. Jamkratoke, M.; Ruangpornvisuti, V.; Tumcharern, G.; Tuntulani, T.; Tomapatanaget, B. *J. Org. Chem.* **2009**, *74*, 3919–3922.
46. Fery-Forgues, S.; Le Bris, M.-T.; Mialocq, J.-C.; Pouget, J.; Rittig, W.; Valuer, B. *J. Phys. Chem. A* **1992**, *96*, 701–710.
47. Hudnall, T. W.; Gabbai, F. P. *J. Am. Chem. Soc.* **2007**, *129*, 11978–11986.
48. Cooper, C. R.; Spencer, N.; James, T. D. *Chem. Commun.* **1998**, 1365–1366.
49. Shen, Y.; Yang, X.-F.; Wu, Y.; Li, C. *J. Fluoresc.* **2008**, *18*, 163–168.
50. Ono, A.; Togashi, H. *Angew. Chem., Int. Ed.* **2004**, *43*, 4300–4302.
51. Liu, J.; Lu, Y. *Angew. Chem., Int. Ed.* **2007**, *46*, 7587–7590.